



Effect of electron irradiation on the optical properties of bismuth doped hafnia-yttria-alumina-silicate fiber

A. V. KIR'YANOV,^{1,2,5} Y. O. BARMENKOV,¹ V. MINKOVICH,¹ S. DAS,³
D. DUTTA,³ A. DHAR,³ M. C. PAUL,^{3,6} S. I. DIDENKO,² S. A. LEGOTIN,²
AND K. I. TAPERO⁴

¹Centro de Investigaciones en Optica, Loma del Bosque 115, Col. Lomas del Campestre, Leon 37150, Mexico

²National University of Science and Technology (MISIS), Leninsky Avenue 4, Moscow 119049, Russia

³Fiber Optics and Photonic Division, Central Glass & Ceramic Research Institute-CSIR, 196, Raja S.C. Mullick Road, Kolkata-700 032, India

⁴Research Institute of Scientific Instruments, Lytkarino, Industrial Zone 'Turaevo' 8, Moscow Region, Russia

⁵kiryanov@cio.mx

⁶paulmukul@hotmail.com

Abstract: We report a study on transformations in absorption and emission spectra of novel bismuth (Bi) doped hafnia-yttria-alumina-silicate fiber, which arise as the result of bombardment by high-energy (β) electrons. Among the featuring data obtained, we reveal substantial growth of 'active' Bi center content in the fiber core-glass with increasing β -irradiation dosage, resulting in dose-dependent intensification of the resonant-absorption bands and enhancement of the emissive potential of the fiber in near-IR, inherent to these centers.

© 2018 Optical Society of America under the terms of the [OSA Open Access Publishing Agreement](#)

OCIS codes: (060.2290) Fiber materials; (160.2750) Glass and other amorphous materials.

References and links

1. A. V. Kir'yanov, "Effects of electron irradiation upon absorptive and fluorescent properties of some doped optical fibers," in *Radiation Effects in Materials* W. A. Monteiro (Ed.) (InTech, 2016).
2. A. V. Kir'yanov, S. H. Siddiki, Y. O. Barmenkov, S. Das, D. Dutta, A. Dhar, V. G. Plotnichenko, V. V. Koltashev, A. V. Khakhalin, E. M. Sholokhov, N. N. Il'ichev, S. I. Didenko, and M. C. Paul, "Hafnia-yttria-alumina-silicate optical fibers with diminished mid-IR ($>2 \mu\text{m}$) loss," *Opt. Mater. Express* **7**(7), 2511–2518 (2017).
3. A. V. Kir'yanov, S. H. Siddiki, Y. O. Barmenkov, D. Dutta, A. Dhar, S. Das, and M. C. Paul, "Bismuth-doped hafnia-yttria-alumina-silica based fiber: spectral characterization in NIR to mid-IR," *Opt. Mater. Express* **7**(10), 3548–3560 (2017).
4. E. M. Dianov, V. V. Dvoyrin, V. M. Mashinsky, A. A. Umnikov, M. V. Yashkov, and A. N. Guryanov, "CW bismuth fibre laser," *Quantum Electron.* **35**(12), 1084–1085 (2005).
5. A. V. Kir'yanov, V. V. Dvoyrin, V. M. Mashinsky, N. N. Il'ichev, N. S. Kozlova, and E. M. Dianov, "Influence of electron irradiation on optical properties of Bismuth doped silica fibers," *Opt. Express* **19**(7), 6599–6608 (2011).
6. R. R. Gonçalves, G. Carturan, L. Zampedri, M. Ferrari, M. Montagna, A. Chiasera, G. C. Righini, S. Pelli, S. J. L. Ribeiro, and Y. Messaddeq, "Sol-gel Er-doped $\text{SiO}_2\text{-HfO}_2$ planar waveguides: A viable system for 1.5- μm applications," *Appl. Phys. Lett.* **81**(1), 28–30 (2002).
7. J. K. Sahu, P. Dupriez, J. Kim, A. J. Boyland, C. A. Codemard, J. Nilsson, and D. N. Payne, "New Yb:Hf-doped silica fiber for high-power fiber lasers," in *Conference on Lasers and Electro-Optics/Quantum Electronics and Laser Science and Photonic Applications Systems Technologies*, Technical Digest (CD) (Optical Society of America, 2005), CTuK1.
8. D. Ramirez-Granados, A. V. Kir'yanov, Y. O. Barmenkov, A. Halder, S. Das, A. Dhar, M. C. Paul, S. Bhadra, S. I. Didenko, V. V. Koltashev, and V. G. Plotnichenko, "Effects of elevating temperature and high-temperature annealing upon state-of-the-art of yttria-alumino-silicate fibers doped with Bismuth," *Opt. Mater. Express* **6**(2), 486–508 (2016).

9. Y. Chu, J. Hao, J. Zhang, J. Ren, G.-D. Peng, and L. Yuan, "Temperature properties and potential temperature sensor based on the Bismuth/Erbium co-doped optical fibers," in *25th International Conference on Optical Fiber Sensors*, Proc. SPIE **10323**, 1032371 (2017).
10. S. Firstov, A. Kharakhordin, S. Alyshev, K. Riumkin, E. Firstova, M. Melkumov, V. Khopin, A. Guryanov, and E. Dianov, "Formation of laser-active centers in bismuth-doped high-germania silica fibers by thermal treatment," *Opt. Express* **26**(10), 12363–12371 (2018).
11. V. V. Dvoyrin, A. V. Kir'yanov, V. M. Mashinsky, O. I. Medvedkov, A. A. Umnikov, A. N. Guryanov, and E. M. Dianov, "Absorption, gain and laser action in bismuth-doped aluminosilicate optical fibers," *IEEE J. Quantum Electron.* **46**(2), 182–190 (2010).

1. Introduction

Exposure a matter to bombardment by nuclear particles is impactful in nuclear industry and space technology as it leads to degradation of critical properties of a nuclear reactor and may jeopardize worthiness of a spacecraft; besides, it may affect health and work safety of the personnel on-duty. Thus, it is hard to overestimate the need of reliable control over dosage of such external radiations as energetic electrons, alpha and gamma particles, protons, etc. in these circumstances.

On the other hand, the effect of bombardment upon versatile properties of optical fiber also presents interest as it is utilizable as a dosage sensor, placed in a reactor's inner/outer parts or onboard of a spacecraft. Modifications of such physical characteristics as absorbance and emissivity of a fiber, during or posterior to bombardment, may be impactful for dosimetry. For radiation-sensing applications, most promising are silica based fibers, easily fabricable and relatively cheap. Among these, fibers doped with rare earths or transitional metals seem to be a relevant choice as such dopants are highly susceptible to nuclear particles in effect of internal ionization of core-glass network. For instance, susceptibility to flow of high-energy (β) electrons was recently studied by us for a variety of doped fibers; see e.g [1]. and references therein.

The current work serves to address a specific effect of β -bombardment upon absorptive and emissive potential of novel aluminosilicate fiber co-doped with Hafnium (Hf), Yttrium (Y), and Bismuth (Bi) (Bi-HYAS) [2,3]. Bi-HYAS fiber is a kind of Bi-doped silica fibers with core co-doped with Alumina (Al) [4], which are promising for telecom applications as capable of lase in the 1.15–1.25- μm region. In such fibers, absorption bands in VIS/NIR (centered at ~ 500 , ~ 700 , ~ 800 , ~ 1000 , and ~ 1400 nm) and broadband NIR emission, covering the 1.0–1.5- μm range, stem from the presence of Bi-related 'active' centers (BACs), associated with Al and Si. Besides, Bi-HYAS fiber demonstrates (because of co-doping with Hf) reduced loss beyond ~ 2 μm [2,3], which is attractive for NIR photonics.

2. Results and discussion

To irradiate Bi-HYAS fiber, we employed a linear accelerator, outputting a beam of β -electrons with a narrow-band spectrum (~ 6 MeV) in a ~ 5 - μs pulsed mode [1,5]. Samples of the fiber, 1–2 m in length, were placed into the accelerator's chamber for growing irradiation doses. Bombardment dosage is exemplified herein by 1×10^{12} , 1×10^{13} , 1×10^{14} , and 1.0×10^{15} cm^{-2} doses (further – '1' to '4'); pristine fiber is designated as '0'. Note that the irradiated fibers were relaxed for ~ 1 month prior to experiments.

Fabrication process of the fibers of HYAS type comprised standard MCVD / solution-doping techniques at the preform stage and conventional drawing [2,3]. The fiber's basic parameters are indicated in Fig. 1.

As seen, the absorption bands in VIS/NIR are typical to BACs, associated with Al and Si. Absorption growth at < 450 nm is inherent to the presence of Hf and indicates rise of scattering loss, explained by partial phase-separation because of inconsistency of sub-lattices formed by Si and Hf atoms and by the presence of non-bridging oxygens (NBOs) [2]. High numerical aperture (~ 0.24), large core diameter (~ 12 μm), and relatively high refractive-index difference (~ 0.02) provide multimode guidance in VIS/NIR, advantageous for the experiments on β -irradiation and measurements of the radiation-induced changes in the fiber.

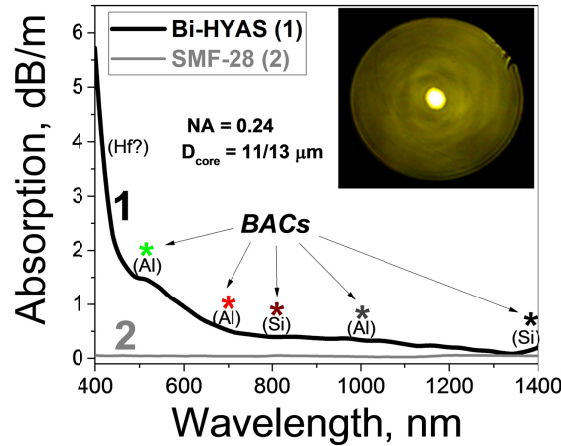


Fig. 1. (main-frame) Attenuation spectra of Bi-HYAS (curve 1) and SMF-28 (curve 2) fibers, measured in VIS/NIR spectral region, with characteristic BACs bands being asterisked and (inset) micro-photograph of Bi-HYAS fiber at WL illumination.

Figure 2(a) demonstrates how white-light (WL) transmission spectra of Bi-HYAS fiber and, for comparison, Bi-free HYAS fiber (with equal amounts of other co-dopants) change with dose (for worthiness of comparison, all samples had the same length in the experiment). Figure 2(b) visualizes the dose dynamics of the fibers darkening (optical microscopy data). Besides, we compare in Fig. 3 the results of irradiation (for maximal dose) upon attenuation in VIS of Bi-HYAS and standard undoped SMF-28 fibers.

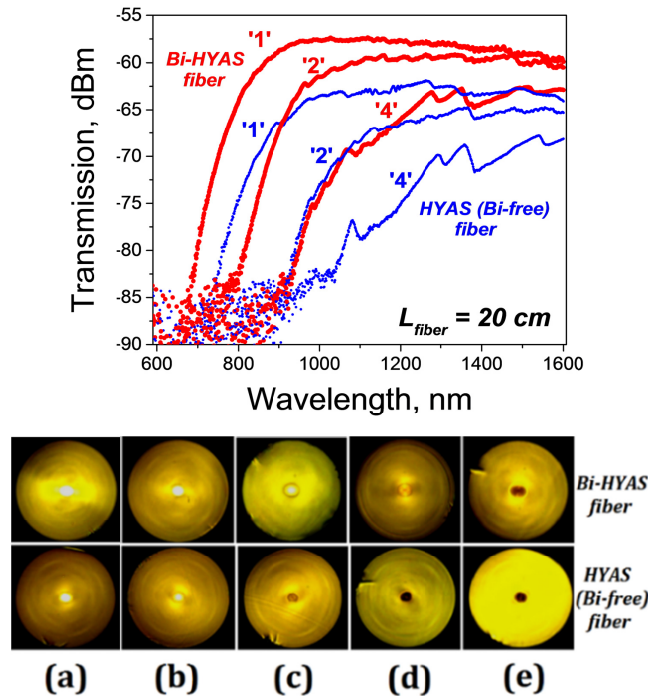


Fig. 2. (top) Transmission spectra in VIS/NIR domain of 20-cm pieces of Bi-HYAS (red curves) and analogous Bi-free HYAS (blue curves) fibers, exemplified for doses '1', '2', and '4'; (bottom) micro-photographs of cleaved ends of these fibers (upper line – Bi-HYAS; lower line – HYAS (Bi-free) fiber), obtained at WL-illumination, in pristine state '0' (a) and after bombardment with doses '1' (b), '2' (c), '3' (d), and '4' (e).

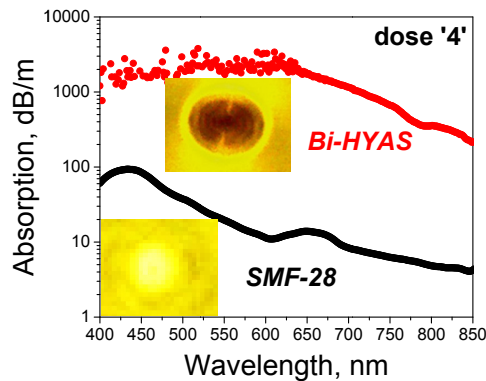


Fig. 3. (main-frame) Attenuation spectra in VIS of Bi-HYAS fiber (red curve) and dopants-free SMF-28 (black curve) fiber, measured after irradiation with dose '4'. (insets) micro-photographs of core-areas of the two fibers, suffered this dose.

First, we reveal from this set of data that Hf, Y, and Bi dopants intensify core darkening after irradiation. This is not surprising as these heavy metallic atoms are strong sources of 'secondary' carriers, generated by 'primary' β -electrons and eventually stabilized by the formation of variety of defect centers with absorption bands in UV/VIS/IR. Second, we notice that the addition of Bi to HYAS core-glass diminishes magnitude and rate of dose-induced absorption (IA) and, also, leads to shifting of its gravity center to anti-Stokes side. This phenomenon probably arises due to the property of Bi atoms to capture a considerable portion of generated carriers with producing a big number of extra BACs (relatively to pristine state) in Bi-HYAS fiber; it appears that this effect competes formation of other defect centers. Clearly, such a scenario does not have matter in 'pure' (Bi-free) HYAS fiber.

Figure 4 shows an interesting detail of β -bombardment, revealed by the data of electron-force microscopy of cleaved end of Bi-HYAS fiber. As compared with pristine state of the fiber (a) and its state after receiving low doses ('1' to '3'; not shown) – where core/cladding interface was kept relatively homogeneous – a drop-like structure arose on the interface after receiving the highest irradiation dose '4' (b). This pattern might have resulted from strong modification of core-glass, suffered the biggest (in our case) dose, produced by internal stresses that might happen in effect of atoms displacement or local heating. We annotate here this feature as it helps to address the abrupt changes in optical properties of Bi-HYAS fiber, occurring after the biggest irradiation dose (see below). Indeed, the morphological transformations on the core/clad boundary (b) ought to lead to light-scattering and so affect the fiber's absorptive and emissive characteristics.

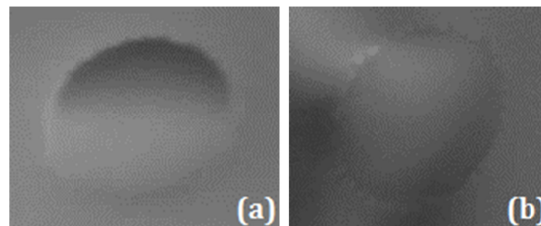


Fig. 4. Micro-images of cleaved ends of core-area of Bi-HYAS fiber samples being in (a) pristine state '0' and (b) after β -bombardment with dose '4'.

In Figs. 5, 6, and 7(a) we resume the basic sides of β -bombardment in terms of transformations in attenuation (absorption) and emission spectra of Bi-HYAS fiber. Besides, in Figs. 7(b), 8, and 9, we make insight into fine details of the phenomena, viz. dose-dependent resonant-absorption bleaching contrast (BC) and non-exponentiality of NIR emission kinetics of BACs at in-band 1060-nm excitation.

The dose-dependent attenuation spectra of fiber samples (with L_f variable from ~ 0.5 to tens cm, depending on dose received) were measured by the cutback method. The dose-dependent emission spectra were obtained at pumping fiber samples (with $L_f = 25\text{--}30$ cm) by a 1060-nm laser diode; note that the pump wavelength matched maximum of $\sim 1\text{-}\mu\text{m}$ absorption band of Al-BACs. NIR emission was detected in ‘backward’ geometry, employing a 2×1 wavelength-division multiplexer (WDM) [3]. NIR emission lifetime was measured in the same geometry; pump light in this case was modulated at frequency 50 Hz and modulated backward emission was detected with a Ge photodetector (200-kHz bandwidth) and oscilloscope. We also measured nonlinear absorption, K_{nl} , of Bi-HYAS fiber at pump wavelength in function of β -dose and pump power, P_{in} . K_{nl} was found applying formula: $K_{nl}(P_{in}) = -\ln(T_{nl})/L_f$, where $T_{nl} = P_{out}/P_{in}$ (P_{out} is a residing part of pump-light power).

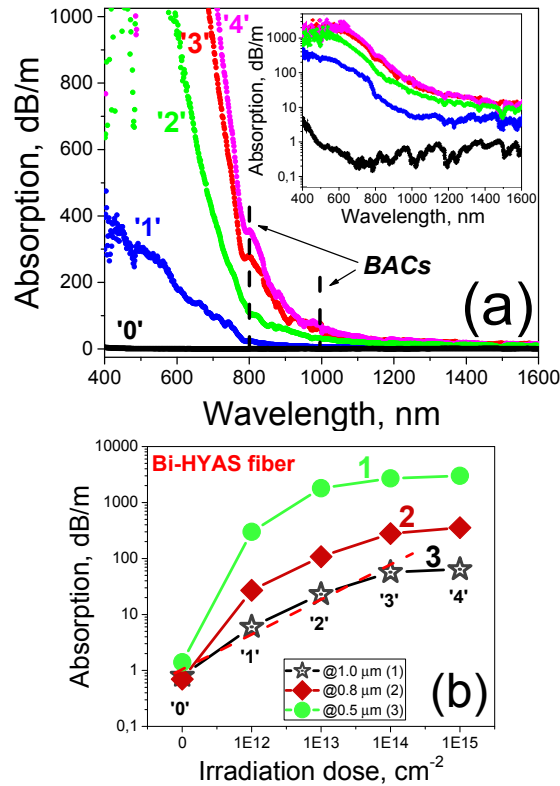


Fig. 5. (a) Attenuation spectra in VIS/NIR of Bi-HYAS fiber in pristine state ('0') and at growing β -irradiation doses '1' to '4' (inset presents the same spectra in logarithmic scale); (b) absorption of Bi-HYAS fiber vs. β -dose in the characteristic domains: ~ 0.5 (curve 1), ~ 0.8 (curve 2), and ~ 1000 (curve 3) μm . In (b), the red dashed line schematizes proportionality between absorption magnitude in the BACs NIR ($\sim 1 \mu\text{m}$) band and β -dose.

As seen from Fig. 5(a), IA-growth in VIS at high doses ('4' and '5') in Bi-HYAS fiber reaches ~ 3000 dB/m (see inset), a much higher value than that accessible in SMF-28 fiber, limited to ~ 100 dB/m (Fig. 3). IA in Bi-HYAS fiber spectrally covers UV/VIS/NIR range and can be assigned to increasing the number of non-bridging oxygen-hole centers (NBOHC) and other defects such as Si-, Al-, Hf-related centers and BACs (via effective re-charging of Bi atoms' proximity at capturing secondary carriers generated at β -bombardment) [5]. The dependences of IA vs. irradiation dose, specified for different spectral regions (~ 0.5 , ~ 0.8 , and $\sim 1.0 \mu\text{m}$), are shown in Fig. 5(b) by curves 1, 2, and 3, respectively. The type of IA-growth in

NIR is perspective for sensing low irradiation doses, see the dashed red line in Fig. 5(b), where attenuation rises in proportion $\sim 0.1 \text{ (dB/m) / cm}^{-2}$.

Figure 6 snapshots, for increasing β -doses, the changes in the emissive potential of Bi-HYAS fiber at excitation into $\sim 1\text{-}\mu\text{m}$ absorption band @1060 nm. As seen, emission beyond $1 \mu\text{m}$, characteristic to Al-related BACs, gets steadily enhanced and broadened up to dose '3' but then, at maximal dose ('4'), drops. These two features, schematized in Fig. 7(a) by the dashed red and yellow lines, are perspective (i) for 'conventional' sensing low doses, proportional to NIR emission power (in proportion $\sim 0.05 \text{ dB / cm}^{-2}$, for $L_f = 30 \text{ cm}$), and (ii) for 'alarmistic' sensing high (say, unacceptable) doses, accumulated in a hazardous place.

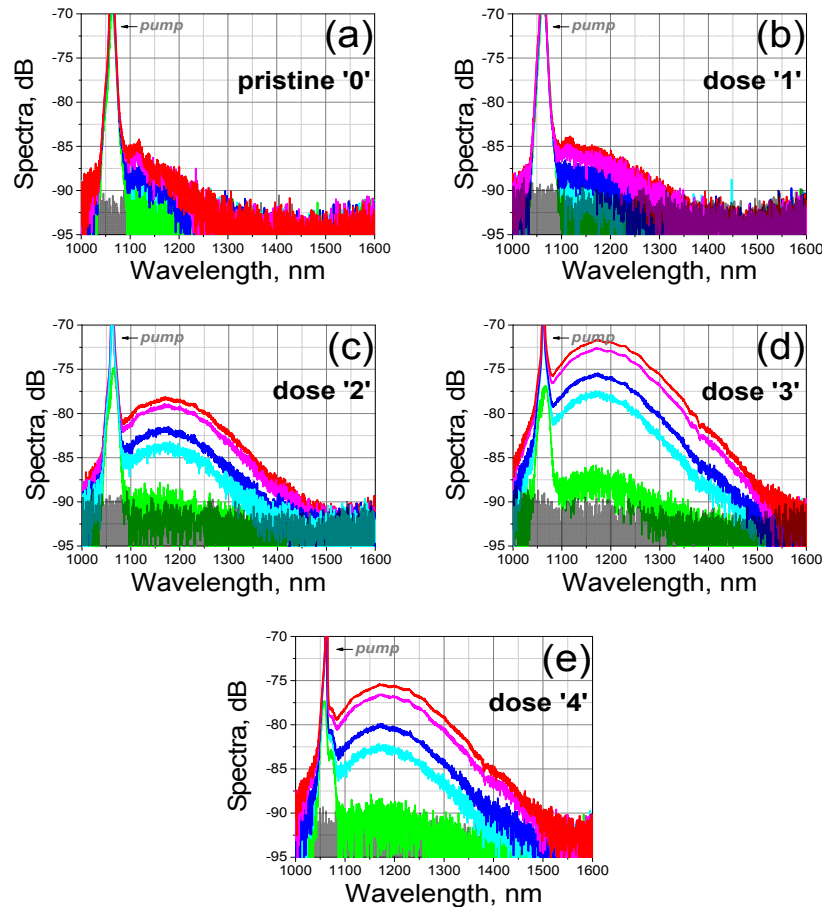


Fig. 6. Emission spectra in NIR of pristine Bi-HYAS fiber (a) and at growing β -irradiation doses '1' (b), '2' (c), '3' (d), and '4' (e); all data are obtained with fiber samples of the same length ($L_f = 30 \text{ cm}$) in the same conditions.

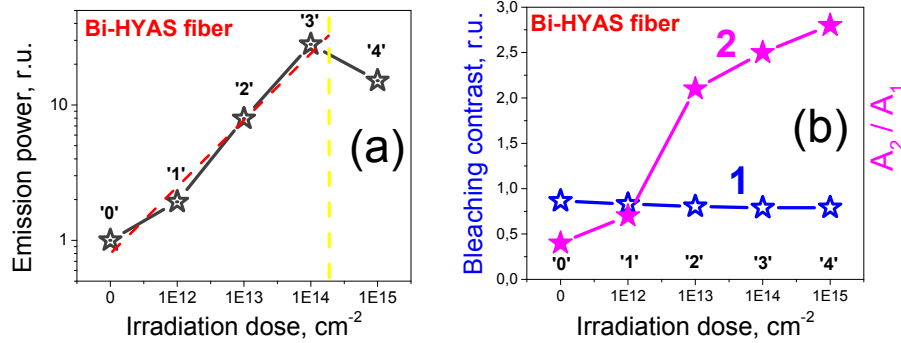


Fig. 7. (a) Dose dependence of relative (to the pristine-state) emission power at $\sim 1.15 \mu\text{m}$. The red line schematizes the proportionality law between BACs-related NIR ($>1.1 \mu\text{m}$) power and irradiation dose whilst the yellow line marks the dose, at which emission growth is suddenly replaced by decrease. $L_f = 30 \text{ cm}$. (b) Dose dependences of BC (curve 1) and amplitude ratio of emission decay (curve 2), fitted by the model of two exponents.

NIR-emission enhancement in Bi-HYAS fiber at increasing β -dose presents news: none similar was found for Hf-free Bi-doped aluminosilicate fiber [5]. Hence, Hf co-doping plays a considerable role in the effect's provenance. Indeed, apart from the sensitizing effect for generating secondary carriers at β -bombardment and so effective producing extra BACs (Fig. 5), Hf atoms enhance flexibility of core-glass network because of abundant NBOs, allowing accommodation of optically-active dopants in almost equivalent environments [6,7] (in our case, Bi atoms and, eventually, BACs); furthermore, Hf doping is favorable as it modifies core-glass structure, facilitating dispersion of the centers. Meanwhile, a partial decrease of NIR emission power at maximal dose '4' may be caused by worsening of core-cladding interface at such high doses, which sources growth of scattering loss (refer to Fig. 4 and the notes therein); another possible reason may be significant rise of loss in NIR at high doses, produced by irradiation-induced inherent defects of core-glass but irrelevant to the presence of Bi / Hf atoms. [Note here that pronounceability of dose-dependent rise of NIR emission in Bi-HYAS fiber also depends on its length used (in Fig. 6, it is exemplified for $L_f = 30 \text{ cm}$): for short fibers, the effect is weaker (apparently, because of small volume of core-glass, subjected to irradiation), whereas, for long pieces of the fiber, it diminishes owing to NIR emission reabsorption in its weakly pumped rear part.]

In Fig. 8, the pattern of nonlinear (bleachable under the action of 1060-nm pump) absorption of Bi-HYAS fiber as function of β -dose is shown. Here, lengths of fibers were chosen to fit back-proportionality to small-signal absorptions (α_0), characteristic to different doses, which ensures comparable optical densities. As pump wavelength matches the right slope of $\sim 1\text{-}\mu\text{m}$ absorption band of Al-BACs (Fig. 1), this permits effective bleaching and small residual, or unbleached, loss (α_F). Besides, the dependence of BC, defined as normalized difference $(\alpha_0 - \alpha_F) / \alpha_0$, on β -irradiation dose is shown by blue curve 1 in Fig. 7(b).

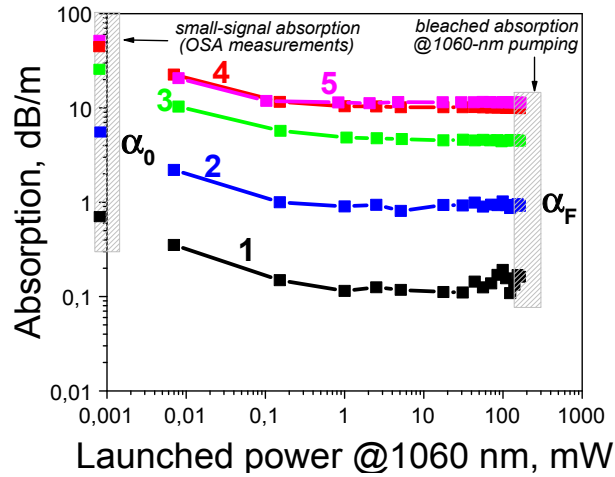


Fig. 8. Nonlinear absorption coefficients of Bi-HYAS fiber in pristine state '0' (curve 1) and after irradiation with doses '1' – '4' (curves 2 – 5), vs. pump power at 1060 nm.

As seen from Fig. 8, the dose-dependent rise of resonant absorption in the BACs $\sim 1\text{-}\mu\text{m}$ band (see curve 3 in Fig. 5(b)) remains bleachable (compare curves 1 to 5 in Fig. 8) with only a slight trend of unbleached background loss to elevate, or, in other words, slight BC worsening, from ~ 0.9 to ~ 0.8 (see curve 1 in Fig. 7(b)). This permits to conclude that, at least for the NIR region, β -bombardment leads to net growth of concentration of 'active' BACs in Bi-HYAS fiber, not to notable increase of unbleached background loss, inherent to defect centers of other – irrelevant to Bi co-doping – types.

These results present interest from a general point of view, demonstrating that irradiating a fiber of Bi-HYAS or similar type by β -electrons provides a mean to substantially increase concentration of NIR emission inherent to BACs (Fig. 7(a)), without worsening of the centers' functionality in terms of BC (see curve 1 in Fig. 7(b)). This effect deserves attention for laser applications as it presents a way to enhance emissivity of Bi-HYAS fiber, in analogy to impact of thermal annealing, known for to Bi-doped fibers of different types [8–10].

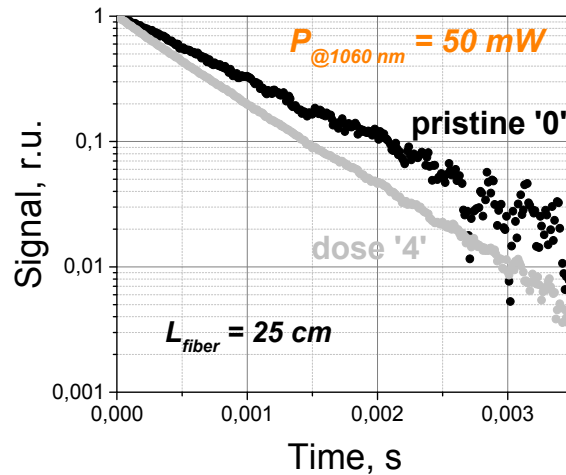


Fig. 9. Normalized NIR emission decays in Bi-HYAS fiber, measured in pristine state '0' (black) and after dose '4' (gray).

In Fig. 9, we exemplify BACs-related NIR-emission kinetics for the two featuring cases: for Bi-HYAS fiber being in pristine state (black curve) and that suffered maximal irradiation

dose '4' (gray curve) (the kinetics for samples passed intermediate doses '1' to '3' fill the gap between these two curves). As seen, NIR emission lifetime shortens but slightly as the result of β -bombardment. [Note here that NIR emission in pristine Bi-HYAS fiber is known to obey a nearly exponential law of decaying at $\sim 1\text{-}\mu\text{m}$ excitation [3], evidencing none or negligible deteriorating processes such as up-conversion or clustering.] This favorably differs Bi-HYAS fiber from Bi-doped Hf-free aluminosilicate analogs.

It is relevant to fit the dose-dependent BACs-emission lifetime, for each dose, by a product of two exponents with decay times $\tau_{1,2}$ and amplitudes $A_{1,2}$, respectively. Such fitting was proceeded for the guess quantity (for each dose) being the longer decay, $\tau_1 = 1.02$ ms (found for pristine Bi-HYAS fiber [3]) to determine τ_2 , A_1 , and A_2 values (at $R^2 > 0.995$). τ_2 -value found in this way lies within $(0.51 \pm 0.05)\text{-ms}$ domain, for either dose. Accordingly, ratio A_2/A_1 (the key output, specifying deviation of kinetics from single exponent), built in function of β -irradiation dose, is shown by magenta curve 2 in Fig. 7(b). As seen from the figure, A_2/A_1 -ratio steadily increases with dosage, which means that the weight of the shorter component in decay (τ_2) becomes bigger than that of the longer one (τ_1). We explain this fact as stemming from the rise of background loss on NIR tails of IA-spectra (Fig. 5(a)), associated to other defect centers produced at β -irradiation, at interaction with which emission-active BACs partially loose excitation via a kind of a non-radiative deexcitation process. In this sense, we cannot disregard a deteriorating role of growing content of BACs joined in pairs or clusters at β -bombardment, which naturally leads to nonexponentiality of emission kinetics [11].

Funding

Ministry of Education and Science (Russian Federation) (K3-2017-015); Department of Science and Technology (DST), Govt. of India, New Delhi.

Acknowledgments

This work was supported via the Increase Competitiveness Program of NUST «MISIS» of the Ministry of Education and Science (Russian Federation) under Grant K3-2017-015 and by the Department of Science and Technology (DST), Govt. of India, New Delhi.